Modulation of Kv Channel Expression and Function by TCR and Costimulatory Signals during Peripheral CD4+ Lymphocyte Differentiation

Qing-Hua Liu,[1] Bernd K. Fleischmann,[2] Brian Hondowicz,[1] Curtis C. Maier,[3] Laurence A. Turka,[4] Katsuyuki Yui,[6] Michael I. Kotlikoff,[5] Andrew D. Wells,[4] and Bruce D. Freedman[1]

[1]*Department of Pathobiology, School of Veterinary Medicine, University of Pennsylvania, Philadelphia, PA 19104*
[2]*Institute für Neurophysiologie, University of Cologne, Cologne D-50931, Germany*
[3]*Department of Safety Assessment, GlaxoSmithKline, King of Prussia, PA 19406*
[4]*Department of Medicine, School of Medicine, University of Pennsylvania, Philadelphia, PA 19104*
[5]*Department of Biomedical Sciences, College of Veterinary Medicine, Cornell University, Ithaca, NY 14853*
[6]*Department of Immunology, Nagasaki University, School of Medicine, Nagasaki, 852-8523, Japan*

Abstract

Ionic signaling pathways, including voltage-dependent potassium (Kv) channels, are instrumental in antigen-mediated responses of peripheral T cells. However, how Kv channels cooperate with other signaling pathways involved in T cell activation and differentiation is unknown. We report that multiple Kv channels are expressed by naive CD4+ lymphocytes, and that the current amplitude and kinetics are modulated by antigen receptor–mediated stimulation and costimulatory signals. Currents expressed in naive CD4+ lymphocytes are consistent with Kv1.1, Kv1.2, Kv1.3, and Kv1.6. Effector CD4+ cells generated by optimal TCR and costimulation exhibit only Kv1.3 current, but at approximately sixfold higher levels than naive cells. CD4+ lymphocytes anergized through partial stimulation exhibit similar Kv1.1, Kv1.2, and/or Kv1.6 currents, but approximately threefold more Kv1.3 current than naive cells. To determine if Kv channels contribute to the distinct functions of naive, effector, and anergized T cells, we tested their role in immunoregulatory cytokine production. Each Kv channel is required for maximal IL-2 production by naive CD4+ lymphocytes, whereas none appears to play a role in IL-2, IL-4, or IFN-γ production by effector cells. Interestingly, Kv channels in anergized lymphocytes actively suppress IL-4 production, and these functions are consistent with a role in regulating the membrane potential and calcium signaling.

Key words: potassium channel • CD28 • patch clamp • superantigen • anergy

Introduction

Immune responses are initiated and regulated by the physical interactions of receptors and ligands on lymphocytes and APCs, and by soluble signaling factors including cytokines and chemokines, which are produced by APCs and inflammatory cells. Therefore, dynamic external factors shape the ongoing responsiveness of T cells, as do intrinsic changes in their physiological state. One important intrinsic determinant of T cell responsiveness is the membrane potassium permeability, which is modulated by potassium channels. Potassium channels play an essential role in immature thymocyte expansion (1) and effector activities of peripheral human lymphocytes (2). Charybdotoxin (CTX)* and margatoxin (MgTX), which block the predominant voltage-dependent potassium (Kv) channel (Kv1.3) of peripheral lymphocytes, depolarize the plasma membrane (3–5), and thereby inhibit TCR-mediated calcium influx (6–8), IL-2 production (9), and proliferation (9, 10). Kv

Abbreviations used in this paper: CFSE, 5-6-carboxyfluorescein diacetate succinimidyl; Cm, membrane capacitance; CTX, charybdotoxin; DTX-I, dendrotoxin-I; DTX-K, dendrotoxin K; Kv channel, voltage-gated potassium channel; MgTX, margatoxin; Vm, membrane potential.

channels also regulate the loss of intracellular K^+, which is a prerequisite step in normotonic or FAS-mediated apoptosis (11–13) and regulatory volume responses to hypotonic (low osmolarity) stress (6). In naive lymphocytes, Kv channels regulate the activation of β-integrins (14), which participate in cellular adhesion and transmigration through the endothelium of venules.

Consequently, any regulation of Kv channel expression or permeation during T cell differentiation could affect their physiological state and functional responses. In fact, the kinetics and amplitude of Kv currents are regulated during murine thymocyte maturation (15–17) and after mitogen stimulation of human (18, 19) and murine peripheral T lymphocytes in vitro (20). Moreover, in vivo administered peptide inhibitors of Kv1.3 suppress delayed type hypersensitivity responses and antigen-specific antibody production in miniswine (21) as well as immune-mediated neurodegeneration in models of experimental allergic encephalitis in the rat (22, 23). These studies collectively suggest that Kv channels regulate physiological functions that define key immunological responses of T cells.

Given the well established role for Kv channels in regulating cell volume, apoptosis, membrane potential, and calcium influx, and the critical role of calcium in T cell differentiation, and IL–2 production in particular, we hypothesized that Kv channels may contribute to the unique physiology and responsiveness of naive and differentiated T cells. To address this hypothesis, we defined the modulation, by TCR and costimulation, of Kv currents in naive, effector, and anergic $CD4^+$ lymphocytes, and the role of each current component in cytokine production. We directly measured the amplitude, kinetic properties, and pharmacology of Kv current in primary murine lymphocytes as well as the contribution of each current component to the steady-state membrane potential. We report that $CD4^+$ T cells express multiple Kv1 (Shaker-related) family potassium channel isoforms and that antigen stimulation in vivo evokes distinct expression patterns in productively primed (effector) and primed nonproliferating (anergic) $CD4^+$ cells. Moreover, Kv channels in naive, effector, and anergic cells each contribute differently to the production of key immunoregulatory cytokines including IL–2, IL–4, and IFN-γ. The mechanism of cytokine regulation by Kv channels corresponds to their role in regulating the membrane potential and calcium signaling in each T cell population.

Materials and Methods

Stimulation of Transgenic $CD4^+$ Lymphocytes In Vivo. The Mls-1^a reactive Vβ8.1 TCR transgenic mouse used in these studies has been described previously (24). Greater than 98% of peripheral T cells in this mouse express a Vβ8.1 TCR transgene. Transgenic T cells were activated in vivo by intravenous inoculation of T lymphocyte–depleted splenocytes (primarily B cells) from CBA/J mice (Mls-1^a positive) that were prepared as described previously (25). In brief, the spleen capsule was disrupted with 22-gauge hypodermic needles allowing the release of lymphocytes. Red blood cells in unfractionated splenocyte prepara-

tions were lysed with Gey's solution. The RBC-depleted preparation was incubated with anti-Thy1 mAb (3O-H12; BD Biosciences) and Thy-1$^+$ cells (T lymphocytes) were depleted by complement (H-2 complement; Pel Freeze) lysis. Transgenic T cells were stimulated by intravenous inoculation of Vβ8.1 TCR transgenic mice with 15 million (in 0.15 ml PBS) T cell–depleted CBA/J splenocytes.

$CD4^+$ Lymphocyte Purification. Inguinal, popliteal, axillary, and submandibular lymph nodes were removed from mice and placed into complete RPMI medium. The lymph node capsule was disrupted with sterile 25-gauge hypodermic needles to release lymphocytes and large debris was removed by filtration through sterile nylon mesh (70 μM pore diameter). The filtered cell suspension was first incubated with monoclonal antibodies (BD Biosciences) against B220 (RA3–6B2), granulocytes (RB6–8C5), Class I MHC (M5/114), and CD8 (Ly-2, 53–6.7). Antibody-stained (non-$CD4^+$) cells were removed by immunomagnetic depletion (Miltenyi Biotec). Alternatively, washed antibody-treated cells were complement killed. Dead cells were removed after complement treatment by centrifugation over a Lympholyte®-M (CEDARLANE Laboratories Ltd.) step gradient. Viable cells were recovered and washed twice in RPMI medium before use in proliferation experiments. The purity of nonstained ($CD4^+$) lymphocytes was determined by flow cytometry. These methods yield a final population that contained at least 95% $CD4^+$ cells.

Cell Culture and In Vitro Stimulation. $CD4^+$ Vβ8.1 TCR transgenic lymph node lymphocytes were stimulated in vitro with Mls-disparate splenocytes or with αCD3 (145–2C11; BD Biosciences). Vβ8.1 $CD4^+$ lymphocytes (5×10^4) and splenocytes (5×10^5 from CBA/J strain, prepared as described above) were cultured together in 0.2 ml DMEM medium containing 100 IU/ml penicillin and streptomycin, 1 mM L-glutamine, 50 μM 2-mercaptoethanol, and heat-inactivated 10% FBS in 96-well flat bottomed plates at 37°C in a humidified environment containing 95%O_2/5% CO_2. Nontransgenic lymphocytes (C57Bl/6) were stimulated in vitro with 1 μg/ml αCD3, 1 μg/ml αCD28 (37.51; BD Biosciences), and APC's to generate effector cells. Anergic cells were generated in vitro by omitting αCD28 Ab and additionally treating with 10 μg/ml CTLA-4 Ig (provided by R. Peach, Bristol-Myers Squibb Pharmaceuticals, Princeton, NJ), again in the presence of APC's. The use of CTLA-4 Ig markedly reduces (∼80%), but does not completely eliminate, proliferation in this in vitro system (due to high strength of TCR signal). However, we find that CTLA-4 Ig induces anergy, defined as a failure to divide or make IL-2 upon restimulation in both the primary proliferating and nonproliferating cells (unpublished observations). The stimulus-dose dependence of proliferation was determined with αCD3 mAb (2C11; BD Biosciences) over a two log concentration range ([μg/ml] 3, 1.0, 0.33, 0.11, and 0.037). All proliferation experiments were performed in triplicate. DNA synthesis was measured in vitro by labeling cells with 1.0 μCi/well [^{3}H]thymidine (NEN Life Science Products) during the terminal 6 h of culture and 48 h of stimulation with αCD3 or 72 h after stimulation with Mls-1^a in vitro.

To determine the proliferative history of T cells in vivo, Vβ8.1 TCR$^+$ transgenic lymph node lymphocytes were labeled with the fluorescent dye 5-6-carboxyfluorescein diacetate succinimidyl ester (CFSE; Molecular Probes), which labels live cells and segregates equally between daughter cells during mitosis, as described previously (26). Lymphocytes labeled with CFSE were injected into Mls-disparate mice (CBA/J) and harvested 2–4 d after inoculation to measure Kv currents and CFSE fluorescence profiles of engrafted $CD4^+$ cells.

Cytokine Measurements. 30 million beads (5-μm–diameter–treated polystyrene; Interfacial Dynamics) were washed and suspended in 0.5 ml PBS. The beads were next incubated with 2.5 μg αIL-2 or αIFN-γ for 2–3 h at 37°C, washed once with complete tissue culture medium, and suspended in 1 ml of culture medium. Cytokine concentrations in culture supernatants were calibrated using rIFN-γ and/or rIL-2 standards. The limit of detection for the IFN-γ and IL-2 standard curves was 195 and 39 pg/ml, respectively. 50 μl of the supernatant to be tested was incubated with 6 μl antibody-coated beads for 1 h at 37°C. The beads were washed with PBS and then incubated with detection antibody for 20 min at room temperature. The beads were washed once and analyzed by flow cytometry.

IL-4 was measured in a standard sandwich ELISA. In brief, 5 μg/ml 11B11 was added to Immulon 2 plates overnight at 4°C. The plates were blocked for 45 min with PBS/10% FBS. 50 μl of the supernatant was added for 1 h at 37°C. The plates were washed with PBS/Tween 20 and biotinylated BVD-6 was added at 1:1,000 for 1 h at 37°C. The plates were washed again and SA-peroxidase was added for 30 min. Finally, the plates were washed, ABTS (KPL) was added, and absorbance (510 nm) was detected at 450 nm excitation.

Electrophysiological Recording. Murine lymph node lymphocytes were stained with fluorescein- or phycoerythrin-conjugated monoclonal antibodies and placed in a recording chamber mounted on an inverted fluorescent microscope (Nikon). Lymphocytes were stained with phycoerythrin-conjugated αCD4 (RM4–5; BD Biosciences) and Vβ8.1 effector (day 3) lymphocytes were additionally incubated with unconjugated 3G11 (BD Biosciences; references 27, 28) followed by FITC-conjugated αIgM (Jackson ImmunoResearch Laboratories). The phenotype of each patched cell was determined before seal formation by direct observation using a fluorescein/phycoerythrin dual filter block (Chroma) and a 40× oil immersion fluorescence objective (Nikon). Patch pipettes with a 4–6-MΩ tip resistance were pulled (Sutter Instrument Co.) from borosilicate glass and were back-filled with solution containing 150 mg/ml nystatin (Sigma-Aldrich). After formation of gigaohm seals (5–10 GΩ), cells were lifted off the chamber bottom and held at −70 mV. Current measurements were initiated when the access resistance decreased to <50 MΩ (∼5–10 min after seal formation). Command potentials were generated and currents were acquired, stored, and analyzed on a personal computer using an EPC-9 amplifier and PulseFit software (Heka). Data were sampled at 3 kHz and recorded on computer disk. For analysis, currents were further filtered at 500 Hz. Unless stated otherwise, macroscopic K^+ currents were elicited with step depolarizations to +50 mV and currents were reported as peak whole cell currents. Current densities were calculated by dividing the peak whole cell current by the cell capacitance. Drugs were applied by direct addition to the bath. The bath solution contained the following (mM): 155 NaCl, 4.5 KCl, 1 $MgCl_2$, 2 $CaCl_2$, 5 Na-HEPES, and 5 glucose, pH 7.2. The pipette solution contained the following (mM): 155 KCl, 1 $CaCl_2$, 1 $MgCl_2$, and 10 K-Hepes, pH 7.2. Recombinant CTX and MgTX were the gift of Maria Garcia (Merck Laboratories, Rahway, NJ) and were also obtained from Alomone Laboratories. Dendrotoxin-I (DTX-I) and dendrotoxin-K (DTX-K) were obtained from Alomone Laboratories.

Pharmacological Identification of Kv Current Components. Kv currents were defined pharmacologically using a variety of toxin inhibitors including CTX (a blocker of Kv1.2, Kv1.3, Kv1.6, and iKCa channels; references 29, 30), DTX-I (a blocker of Kv1.1,

Kv1.2, and Kv1.6 channels; reference 31), DTX-K (a blocker of Kv1.1 channels; reference 32), and MgTX (a blocker of Kv1.1, Kv1.2, Kv1.3, and Kv1.6 but not IK_{Ca}) to define the identity of K^+ currents expressed by naive and primed CD4+ lymphocytes. Because the only CTX-sensitive DTX-I–insensitive Kv channel is Kv1.3, Kv1.3 was identified by first adding DTX-I, which blocks Kv1.1, Kv1.2, or Kv1.6, and then CTX to block Kv1.3. In some experiments, Kv1.1 currents were identified with DTX-K, which is selective for Kv1.1. In these cases, any remaining DTX-K–insensitive, DTX-I–sensitive Kv current is encoded by Kv1.2 and/or Kv1.6. Because Kv1.2 and Kv1.6 are also sensitive to CTX and specific blockers for either of these channels have not been isolated, RT-PCR was used to determine whether Kv1.2 or Kv1.6 mRNA is expressed in lymphocytes, as described below.

Membrane Potential Measurements. CD4+ lymphocytes were identified as described above and membrane voltage was measured directly using the current clamp configuration of the nystatin perforated patch-clamp technique. Whole cell Kv currents were elicited after establishment of electrical access to the cytoplasm to confirm the cells differentiation state and viability. The membrane potential was measured in cells that exhibited the appropriate Kv current phenotype using the voltage clamp recording mode. The role of Kv channels, defined in voltage-clamp experiments, in setting the steady-state potential was determined by sequentially blocking Kv1.1, Kv1.2, and Kv1.6 (with DTX-I), Kv1.3 (with MgTX), and calcium-activated K (KCa) channels (with CTX) as described above.

Intracellular Calcium Measurements. Lymphocytes were loaded with the cell permeant calcium indicator fura-2 AM (3.0 μM; Molecular Probes) in RPMI medium for 15 min at room temperature (25°C). During the final 10 min of fura-2 loading biotinylated αCD3 and αCD4 mAb were added to lymphocyte suspensions. Cell suspensions were placed into the recording chamber on an inverted fluorescent microscope (Nikon) and allowed to adhere to 10 μg/ml poly-L-lysine (Sigma-Aldrich) treated coverslips for 5 min. Excess extracellular fura-2 AM and unbound antibody was washed from the microscope recording chamber with extracellular bath solution, which consisted of the following (mM): 155 NaCl, 4.5 KCl, 2 $CaCl_2$, 1 $MgCl_2$, 5 glucose, and 10 HEPES, pH 7.4. Discrete bandwidth excitation light (340 ± 10 nm, 380 ± 10 nm) from a xenon source coupled to a computer-controlled monochromator (TILL; Applied Scientific Imaging) was delivered to the epifluorescence attachment of the microscope through a quartz fiber optic guide. Excitation light was directed through the fluorescent objective (100×; Nikon) via a dichroic mirror. The emitted fluorescence from fura-2–loaded cells was passed through a 470-nm–long pass filter and images were obtained with an intensified charge-coupled video camera (model C2400–68; Hammamatsu) connected to the side port of the inverted microscope. Four fluorescent video images were averaged and digitized (0.5 Hz) with a video frame grabber (Matrox) using Metafluor acquisition and analysis software (Universal Imaging). Stored images were analyzed offline using the Metafluor package. Within cursor-defined areas of interest paired 340/380 images were background subtracted and the ratio was calculated. The absolute ratio values in the cursor-defined areas were exported into Microsoft Excel and converted to [Ca^{2+}] (33). Calibration factors, R_{max} (340:380 ratio obtained in presence of 5 μM ionomycin and 10 mM Ca^{2+}), R_{min} (340:380 ratio in presence of 5 μM ionomycin and excess EGTA), and $F380_{max}$ and $F380_{min}$ (minimum 510 nm emission with 380 nm excitation) were determined in situ.

RNA Preparation and RT-PCR. Total cellular RNA was prepared according to the acid guanidinium method (34). Genomic DNA was removed from RNA preparations by treating them with DNase I (Boehringer) before cDNA synthesis with Superscript II reverse transcriptase (Life Technologies). PCR was used to amplify cDNA prepared from murine thymocyte RNA. Unique complementary oligonucleotide primer pairs were synthesized to unique 3′ regions of Kv1.1 (sense, bases 979–1007, ATCTTCAAACTCTCCCGCCACTCCAAGGG; antisense, bases 1495–1476, TTGCTTTTTAAACATCGCT; Probe, bases 1292–1321, CTTAGCCTCTGACAGTGACC of the clone MK1; reference 35), Kv1.2 (sense, as above; antisense bases 1667–1648 of cDNA clone RK2, ATATTCTGTGTTCTAAATCA; Probe, bases 1372–1391 of RK2, TACATGGAGATACAGGAGGG; (36), Kv1.3 (sense, as above; AS bases 1538–1521 of clone KV3, ACTTCAACTACTTCTACCACCG; Probe, bases 1315–1336 of clone KV3, TTGGGGTTATTGTTCGTG (37), and Kv1.6 (sense, as above; antisense, bases 1555–1536 of clone KV2, GATGTGGAGTTGGAAGGTAG; Probe, bases 1432–1451 of clone KV2, TATACCCACGTCACTTGTGG (37). The specificity of each of these oligonucleotide primer pairs was confirmed in test PCR reactions using the appropriate mouse cDNA clone as a template (unpublished data). PCR products were separated by electrophoresis in a 2% agarose gel and were capillary blotted onto Genescreen Plus nylon membrane (NEN Dupont) in 0.4 M NaOH and 1.0 M NaCl. DNA probes were 5′-end labeled with γ-[^{32}P]ATP using T4 polynucleotide kinase according to the manufacturer's protocol (Life Technologies).

Results

Voltage-dependent Potassium Currents Expressed by CD4^{+} Lymphocytes In Vivo. To determine whether Kv currents are modulated by antigen stimulation of CD4^{+} lymphocytes, we used an Mls-superantigen–specific Vβ8.1 TCR transgenic mouse model to generate both anergized and productively primed effector cells in vivo. In these mice, superantigen induces a large proportion of CD4^{+} lymphocytes to enter the cell cycle and proliferate, and the resulting expansion is evident as a large increase in CD4^{+} cells within 2–3 d. T cells isolated on day 3 contain productively primed cells that are identified ex vivo according to their expression levels of a disialoganglioside antigen termed 3G11 (Fig. 1 A). 3G11 expressed on naive T lymphocytes is irreversibly down-modulated from the membrane of productively primed effector T cells (27, 28). Importantly, 2 wk after the initiation of an immune response with superantigen in Vβ8.1 TCR^{+} mice, virtually all surviving CD4^{+} T cells, which express 3G11, are anergic by virtue of a diminished capacity to produce IL-2 and proliferate (Fig. 1 B; reference 24).

Kv channels in naive and in vivo primed CD4^{+} T cells were maximally activated with a large step depolarization (120 mV) from the holding potential (−70 mV; Materials and Methods) and currents were dissected with isoform-selective Kv channel peptidyl blockers as described in Materials and Methods. Naive CD4^{+} TCR transgenic cells express small amplitude Kv currents (peak amplitude = 51.0 ± 4.3 pA, $n = 11$; Fig. 2 A). Approximately 50% of the evoked current of naive cells is blocked by 100 nM CTX, whereas the remaining CTX-resistant current in naive CD4^{+} cells (21.4 ± 4.7 pA, $n = 8$) is sensitive to DTX-I inhibition. Similar results are obtained regardless of the order of blocker addition (unpublished data) and in either case, neither toxin-defined current component exhibits significant time-dependent inactivation. The fractional current level after a 250-ms voltage step depolarization is nearly identical to the initial peak current (0.95 ± 0.02,
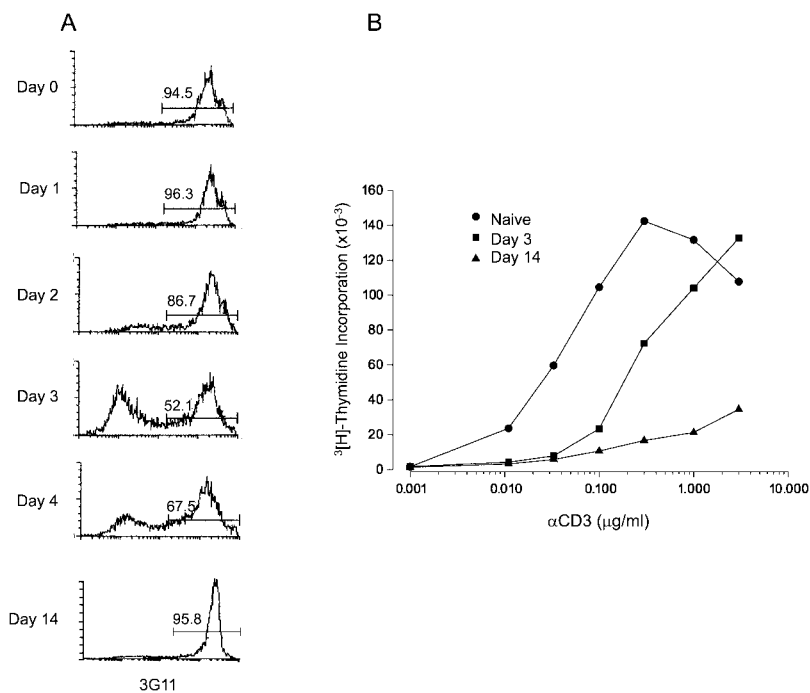

Figure 1. Functional characterization of CD4^{+} Vβ8.1 lymphocytes. FACS® analysis was performed to determine the percentage of 3G11 expressing CD4^{+} cells on indicated days after inoculation. (A) The percentage of 3G11^{+} lymph node lymphocytes decreases during the first few days after Mls-1[a] superantigen inoculation and maximum steady-state number and percentage (∼50%) of 3G11^{−} cells is observed on day 3 after antigen inoculation, after which the proportion of CD4^{+} 3G11^{−} cells progressively decreases. (B) CD4^{+} lymph node lymphocytes from control Vβ8.1 TCR transgenic mice or from mice stimulated with Mls-superantigen in vivo were restimulated with soluble αCD3 mAb (145–2C11) and splenic APC's in vitro. Proliferation was assessed by measuring the amount of [^{3}H]thymidine (counts per minute) incorporation on day 4 of culture for naive and cells previously primed in vivo for 3 (■) or 14 (▲) days. The proliferative capacity of day 14 lymphocytes was markedly decreased. Each value is the mean (±SD) of triplicate cultures and the experiment shown is typical of three similar experiments.

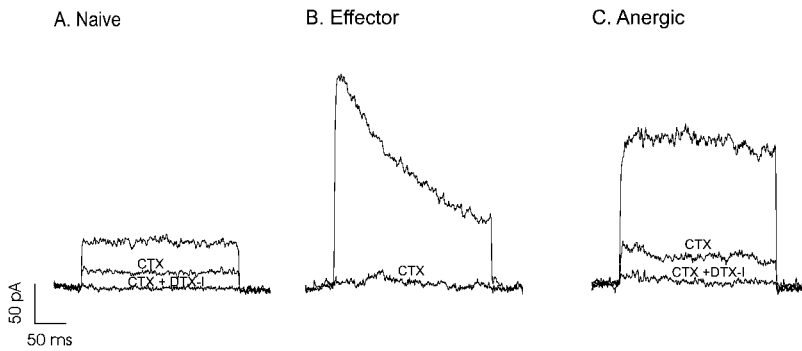**A. Naive**   **B. Effector**   **C. Anergic**

Figure 2. Voltage-dependent potassium currents expressed by antigen specific lymphocytes in vivo. Kv currents were evoked with voltage step depolarizations from -70 to $+50$ mV for 250 s in phenotypically defined CD4$^+$ lymph node lymphocytes. Effector and anergic lymphocytes were produced in vivo by inoculation of Vβ8.1 Tg$^+$ mice with Mls-disparate splenocytes and responder cells isolated as described in Materials and Methods. Whole cell Kv current components were pharmacologically defined with CTX (100 nM) or CTX (100 nM) + DTX-I (100 nM) in naive/unprimed (A), productively primed effector (B), and anergized (C) CD4$^+$ cells. The latter two populations were isolated on days 3 and 14 after inoculation of Vβ8.1 TCR transgenic mice with Mls-superantigen reactive B cells. Each series of recordings is representative of at least eight separate experiments.

$n = 10$). The amplitude and pharmacology of Kv currents in CD4$^+$ lymphocytes from the background mouse strain (CBACa) are quantitatively (30.0 ± 1.3 pA, $n = 3$) and qualitatively similar (unpublished data).

As indicated above, antigen inoculation decreases 3G11 expression on $\sim$50% of CD4$^+$ lymphocytes in Vβ8.1 transgenic mice within 2–3 d (Fig. 1 A), which corresponds to the time of peak proliferative expansion. Because not all cells proliferate in vivo, productively primed cells were identified first by size. The membrane capacitance, obtained with the patch clamp, was used to quantify the cell surface area (volume) in productively primed/proliferating cells, and 3G11$^-$ cells uniformly possess a large membrane capacitance. In fact, the membrane capacitance of 3G11$^-$ CD4$^+$ cells is significantly larger than 3G11$^+$ CD4$^+$ cells isolated after antigen inoculation in vivo (next section). In contrast to naive T cells, productively primed CD4$^+$ Vβ8.1 TCR transgenic lymphocytes (day 3 3G11$^-$) generated in vivo express a larger (3–4 fold) amplitude Kv current (167.0 ± 20.8 pA, $n = 15$), which exhibits prominent time (Fig. 2 B), use-, and voltage-dependent inactivation (unpublished data) at clamp potentials positive to 0 mV. The fractional steady-state current remaining after a 250-ms depolarization is <50% of the peak current (0.43 ± 0.07, $n = 11$). Most significantly, the entire Kv current of productively primed CD4$^+$ lymphocytes is sensitive to CTX inhibition, and no measurable CTX-resistant (DTX-K or DTX-I–sensitive) current (see Fig. 5 B) is expressed.

Subsequent to the period of peak proliferative activity ($\sim$3 d) in vivo, the absolute number and proportion of productively primed (3G11$^-$) Vβ8.1 TCR Tg CD4$^+$ cells decreases progressively and few can be found after 14 d of stimulation in this model. Although a significant number of CD4$^+$ (3G11$^+$) cells persist at 2 wk, these cells exhibit an impaired ability to proliferate ex vivo (Fig. 1 B) on stimulation with anti-CD3 mAb. This inability to proliferate appears to result from a defect in the capacity to produce IL-2 because these anergic cells will respond to exogenous cytokine (38). Importantly, Kv currents measured in anergic (day 14, 3G11$^+$) T cells are quantitatively and qualitatively distinct from those in naive and productively primed cells. Compared with naive cells, the

peak current amplitude in anergic cells is larger (93.6 ± 13.3 pA, $n = 16$) due to an increase in CTX-sensitive (Kv1.3) current (96.0 ± 19.6 pA, $n = 8$, versus 44 ± 6.9, $n = 8$ pA in naive cells), and anergic cell currents exhibit some degree of time-dependent inactivation (Fig. 2 C). The fractional current in anergized lymphocytes following a 250 ms depolarization is 0.77 ± 0.05 ($n = 16$), which is more than naive but less than productively primed effector cells. However, like naive cells anergic cells also express a DTX-I–sensitive (Kv1.1, Kv1.2, and/or Kv1.6) current component.

Kv Current Density of Naive and Primed Lymphocytes. Because lymphocytes enlarge as they progress through the cell cycle, TCR-induced increases in whole cell Kv current levels might simply reflect homeostatic regulation of the plasma membrane channel density. To determine how the increase in peak Kv current amplitude in Mls-superantigen–stimulated lymphocytes relates to the increase in surface area of stimulated cells, peak current values were normalized to the membrane capacitance (C_m), which is proportional to the cell surface area, to obtain a quantitative measure of current (channel) density. The mean C_m was 1.26 ± 0.06 pF ($n = 12$) for unstimulated, 1.86 ± 0.11 pF ($n = 20$) for day 3 CD4$^+$ 3G11$^-$, and 1.69 ± 0.06 pF ($n = 15$) for day 14 (anergized) CD4$^+$ (3G11$^+$) cells. Incidentally, the low capacitance (small volume) of day 3 3G11$^+$ cells (1.37 ± 0.15 pF, $n = 7$) is consistent with the premise that these are not productively primed. Interestingly, naive (1.40 ± 0.06 pF, $n = 16$), day 3 (1.52 ± 0.06, $n = 12$), and day 14 (1.44 ± 0.07, $n = 14$) CD8$^+$ cells from Vβ8.1 TCR Tg mice exhibited no significant capacitance differences.

Capacitance (surface area) normalized toxin-defined current values (Kv current density) were found to be significantly ($P < 0.05$) higher in productively primed effector and anergic lymphocytes than in naive cells ($\sim$2.3 times and 1.4-fold respectively; Fig. 3). The observed differences in total current primarily reflects an increase in CTX-sensitive current density (28.9 ± 2.7 pA/pF, 112.4 ± 18.5 pA/pF, and 42.7 ± 10.6 pA/pF for naive, effector, and anergic cells, respectively). By contrast, the CTX-resistant DTX-I–sensitive current density is essentially identical for resting and anergic CD4$^+$ lymphocytes ($20.9 \pm$
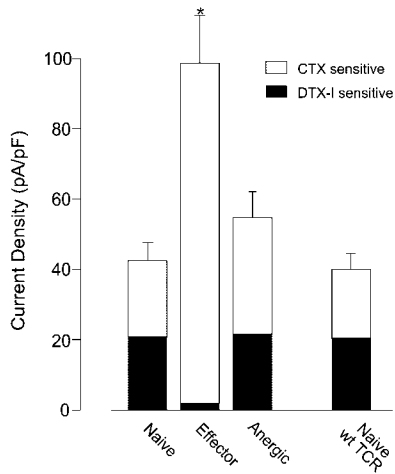
Figure 3. Kv current density in naive, effector, and anergic lymphocytes. Whole cell potassium currents were normalized to the cell surface area (density) for multiple separate experiments (at least 10 measurements for each condition) to determine whether the increase in Kv current is proportional to the increased cell surface area in stimulated lymphocytes. Effector and anergic lymphocytes were produced in vivo by inoculation of Vβ8.1 TCR Tg mice with Mls-disparate splenocytes and T cells were isolated as described in Materials and Methods. The current density of proliferating (day 3, 3G11⁻) lymphocytes (97 ± 15 pA/pF) was ∼2.5-fold greater than the aggregate current density of resting cells, that represents a 6–7-fold increase in CTX-sensitive current density. The CTX-resistant current density for resting and day 14 lymphocytes is similar, whereas the CTX-sensitive current density is about twofold greater in day 14 than naive cells. The current in proliferating cells was significantly larger than any other subpopulation. *, $P < 0.05$.

4.3 pA/pF and 21.7 ± 3.9 pA/pF, respectively). Importantly, the increase in Kv current density is about fourfold greater (455 ± 197 pA/pF, $n = 4$) for CD4⁺ Vβ8.1 TCR transgenic lymphocytes that are inoculated into CBA/J mice compared with those stimulated in Vβ8.1 TCR transgenic mice by injection of superantigen. Consequently, the larger Kv currents in productively primed and anergic lymphocytes are not simply a function of increased cell size or membrane surface area.

Regulation of Kv Currents by Strength of TCR Stimulation and Costimulation. We next examined the regulation, by TCR stimulation and CD28 costimulation, of Kv currents in CD4⁺ T cells. Naive nontransgenic cells (C57Bl/6 mice), like TCR transgenic cells, express a small amplitude Kv current (peak amplitude = 46.2 ± 8.0 pA, $n = 6$)

comprised of DTX–I–sensitive, and DTX–I–resistant, CTX-sensitive components (Fig. 4 A). Because DTX–I inhibits Kv1.1, Kv1.2, and Kv1.6, we examined the effects of the Kv1.1-selective inhibitor DTX–K, which blocks a small fraction of DTX–I–sensitive Kv current in naive cells (22%, $n = 6$; unpublished data). Effector cells were produced in vitro by stimulating naive cells with soluble αCD3 and αCD28 antibodies in the presence of nonpurified splenocytes (APC's) to provide costimulation and antibody cross-linking. Effector cells produced in this way exhibit relatively large amplitude Kv currents (374 ± 48 pA, $n = 11$), which are insensitive to DTX–I or DTX–K (unpublished data), but are completely blocked by CTX (Fig. 4 B) or MgTX (unpublished data). Finally, anergic cells were generated by priming naive cells with αCD3 (no αCD28) and APCs, and by blocking B7-mediated costimulatory signals with CTLA-4 Ig. Costimulatory blockade does not prevent the TCR-mediated increase in peak Kv current levels compared with effector cells (peak current = 406.8 ± 74.9 pA, $n = 11$), but it does affect the current composition. Anergized cells, unlike effector cells, express a DTX–I–sensitive current component (Fig. 4 C). A fraction (11%) of the DTX–I–sensitive Kv current of anergized lymphocytes, like the similar current in naive cells, is sensitive to DTX–K (45.6 ± 13.1 pA, $n = 8$). The remaining (DTX–K–resistant) current in anergic cells is comprised of DTX–I (75 ± 26 pA, $n = 5$) and CTX- (335 ± 65 pA, $n = 3$) sensitive components. Thus, the loss of all DTX-sensitive current and an increase in CTX-sensitive Kv current is associated with productive stimulation of naive CD4⁺ cells, whereas costimulatory blockade in vitro results in an increase in CTX-sensitive Kv current, and failure to down-modulate expression of DTX-sensitive current components.

The consistently larger Kv current amplitude observed in CD4⁺ cells stimulated with αCD3 and αCD28 suggested that Kv channel expression levels might be regulated by the strength or "dose" of antigen. To address this hypothesis, in vivo, Vβ8.1 TCR transgenic lymphocytes were adoptively transferred into Mls-disparate (CBA/J) mice in order to increase the stimulator/responder (CBA/J:Vβ8.1 TCR Tg) cell ratio. By contrast with experiments in which a limited number of stimulator cells are introduced into Vβ8.1 transgenic mice, this approach introduces Vβ8.1 responders into an environment (host) in
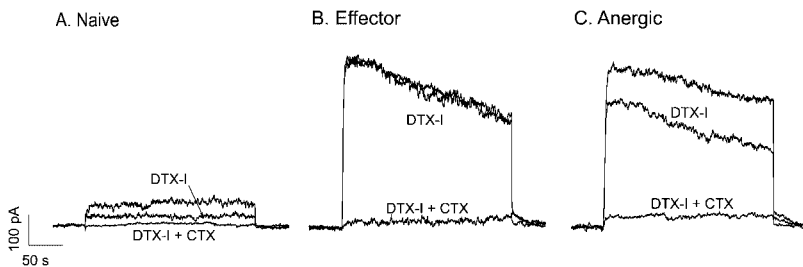

Figure 4. Voltage-dependent potassium currents expressed by CD4⁺ Vβ8.1 TCR transgenic lymphocytes in vitro. Kv currents were evoked in voltage-clamped CD4⁺ lymph node lymphocytes with 250-ms duration voltage step depolarizations from −70 to +50 mV. The Kv current pharmacology was determined for CD4⁺ lymphocytes with 100 nM DTX-I or 100 nM DTX-I and 100 nM CTX in naive T cells (A), or cells stimulated for 3 d in culture with 1 μg/ml αCD3 mAb and 1 μg/ml αCD28, or 1 μg/ml αCD3 mAb and 10 μg/ml CTLA-4 Ig in the presence of APC's to generate proliferating/effector (B) or anergic (C) populations of cells, respectively. CD4⁺ lymphocytes were identified in situ for patch-clamp measurements as described in Materials and Methods.

which nearly every cell expresses the reactive superantigen. Before engraftment, transgenic lymphocytes were labeled with CFSE, so that their proliferative activity in vivo could be assessed retrospectively. The CFSE profile of CD4$^+$ cells isolated after adoptive transfer indicates that most CD4$^+$ cells divide at least three times during the first 2 d of engraftment (Fig. 5 A). Surprisingly, the Kv current (DTX I-insensitive, CTX-sensitive) of CFSE$^+$ CD4$^+$ lymphocytes isolated 2 d after adoptive transfer is ~25-fold larger (741 pA $\pm$ 243 pA, $n = 4$; Fig. 5 B) than currents in naive cells, and 4–5-fold larger than those in CD4$^+$ cells activated with superantigen in Vβ8.1 TCR transgenic mice (Fig. 2 B) or with anti-CD3 and anti-CD28 in vitro (Fig. 4 B).

Molecular Identity of Kv Currents in Resting and Anergic CD4$^+$ Vβ8.1 TCR Transgenic Lymphocytes. A limited subset of all Kv channels (Kv1.1, Kv1.2, Kv1.3, and Kv1.6) exhibit CTX and/or DTX sensitivity. Because these toxins individually, or in combination with one another, block all Kv currents in naive, effector, and anergic CD4$^+$ ce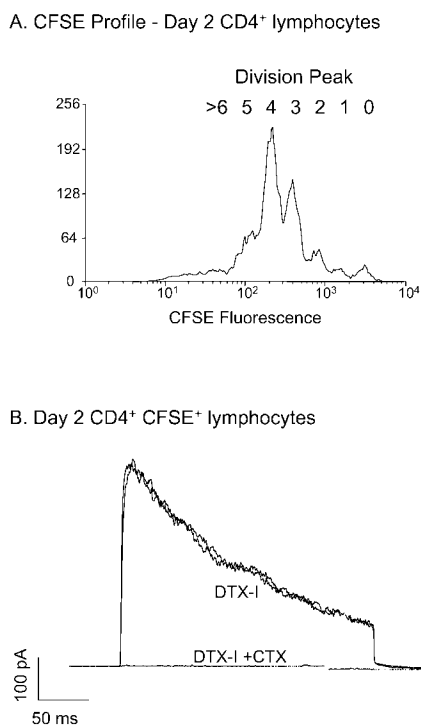lls (Figs. 2, 4, and 5 B), the currents must be encoded by one or more of these four genes. A pharmacological analysis of Kv currents was conducted to make as many definitive identifications as possible. For example, Kv1.3 is the only known DTX-I–resistant CTX-sensitive Kv channel and Kv1.1 is the only known DTX-K–sensitive channel. In contrast, Kv1.2 and Kv1.6 currents cannot be distinguished from one another using available blockers because both are sensitive to DTX-I and CTX and neither is sensitive to DTX-K. Consequently, the DTX-K–resistant DTX-I–sensitive Kv current in naive and anergic CD4$^+$ cells could be encoded by either gene. In fact, RT-PCR analysis revealed that mRNA for all known CTX- and DTX-sensitive Kv channels (Kv1.1, Kv1.2, Kv1.3, and Kv1.6) is expressed in murine CD4$^+$ T cells (Fig. 6).

Coupling of Kv Channels to IL-2 Production in Naive CD4$^+$ Lymphocytes. It is well established that a CTX-sensitive Kv current (Kv1.3) underlies IL-2 production and proliferation of naive human T cells (7, 9), although the functions of Kv channels during secondary immune responses in vivo or in vitro are unknown but likely to be distinct (21, 22). We first tested the role of Kv channels during antigen-mediated proliferative responses of naive CD4$^+$ T cells in vitro to determine whether these murine models recapitulate previous findings with human T cells. Naive CD4$^+$ Vβ8.1 TCR lymphocytes were stimulated with Mls-1^a (irradiated CBA/J splenocytes) alone, as described in Materials and Methods, and [^{3}H]thymidine incorporation was used to measure the extent of DNA synthesis. This superantigen stimulation protocol typically induces a 50-fold increase in [^{3}H]thymidine incorporation into DNA above the background response to control Mls nondisparate (CBA/Ca and Mls-1^b) cells. Importantly, both CTX and DTX-I inhibit these in vitro responses (Fig. 7). Although CTX reduced peak [^{3}H]thymidine incorporation by 25%, CTX and DTX-I together exerted a greater inhibitory effect (~50%) than either blocker alone, indicating that multiple Kv channel isoforms expressed by CD4$^+$ lymphocytes regulate antigen-mediated responsiveness in vitro.

We next examined the mechanism by which blockers might inhibit proliferation, and specifically tested the role of each Kv current in the production of IL-2. Naive CD4$^+$
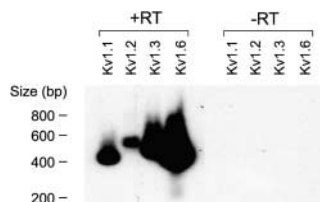
A. CFSE Profile - Day 2 CD4$^+$ lymphocytes

B. Day 2 CD4$^+$ CFSE$^+$ lymphocytes

Figure 5. Proliferative capacity and Kv currents of adoptively transferred Vβ8.1$^+$ CD4$^+$ lymphocytes. CFSE labeled Vβ8.1 TCR transgenic lymph node lymphocytes were inoculated into Mls-disparate (CBA/J) hosts and were subsequently recovered (48 h after inoculation) to analyze the proliferative history and Kv current phenotype of stimulated cells. (A) The CFSE profile of inoculated CD4$^+$ lymphocytes, determined by flow cytometry, demonstrates that the mean proliferative capacity of CD4$^+$ lymphocytes stimulated for 2 d in vivo was ~10 (daughters) per responding T lymphocyte and this reflects an average of three to four cell divisions. The responder frequency was 73.6% in this experiment. (B) Patch-clamp measurements of currents from the same population of CD4$^+$ CFSE$^+$ lymphocytes demonstrate a large amplitude Kv current, which is insensitive to DTX-I (100 nM) but is completely blocked by CTX (100 nM).

Figure 6. Kv channel mRNA expression in CD4$^+$ VB8.1 TCR transgenic lymphocytes. RT-PCR was used to detect mRNA that encodes CTX- and DTX-I–sensitive potassium channels (Kv1.1, Kv1.2, Kv1.3, and Kv1.6; Materials and Methods) in CD4$^+$ Vβ8.1 TCR transgenic lymphocytes. This autoradiograph demonstrates that Kv1.1, Kv1.2, Kv1.3, and Kv1.6 mRNA are expressed in naive cells. Because Kv channel genes are intronless (37, 48), we determined that these products were not amplified from contaminating genomic DNA, which could be present in the lymphocyte RNA preparations. In the absence of the reverse transcription step, PCR products of Kv1.1, Kv1.2, Kv1.3, or Kv1.6 were not amplified from lymphocyte mRNA preparations.
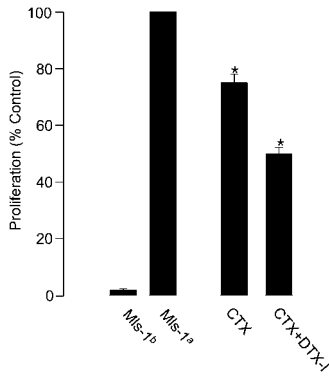
Figure 7. Potassium channel blockers inhibit antigen-mediated proliferation of CD4^{+} Vβ8.1 TCR transgenic lymphocytes. Mls-superantigen–stimulated proliferative responses of CD4^{+} lymphocytes was assessed in vitro by measuring [³H]thymidine incorporation into DNA on day 4 of culture. Purified Vβ8.1 TCR transgenic CD4^{+} lymphocytes were stimulated with irradiated Mls-disparate (CBA/J) splenocytes (stimulator/responder ratio = 10). Each bar represents the mean (±SEM) [³H]thymidine count from at least nine separate experiments. Each value is expressed as a percentage of the control proliferative response obtained in the absence or presence of CTX (100 nM) and/or DTX-I (100 nM) for each individual trial. The mean [³H]thymidine incorporation for all control experiments was 24,845 ± 4,349 cpm (n = 12). *, Mean value is significantly different from control response (P < 0.05). Non Mls-disparate stimulator cells (Mls-1[b], CBACa) did not induce a proliferative response in CD4^{+} Vβ8.1 TCR transgenic lymphocytes.

Figure 8. Effect of Kv channel blockers on IL-2 production by naive CD4^{+} lymphocytes in vitro. Naive CD4^{+} lymphocytes from C57Bl/6 mice were stimulated (in the presence of APCs) with soluble αCD3 (1 μg/ml) and αCD28 (1 μg/ml) in complete RPMI medium. Supernatants were collected between 16 and 18 h after stimulation and assayed for [IL-2] as described. Anergic cells were generated by omitting αCD28 and including CTLA-4 Ig (10 μg/ml) at the initiation of culture. Cells were preincubated for at least 30 min with toxins before stimulation. All data represent the mean of (±SD) of at least three separate experiments, each performed in duplicate. When indicated, the results are significantly different: *, P < 0.05.

lymphocytes, stimulated with plate immobilized anti-CD3, were cultured in the absence or presence of CTX (to block Kv1.3, Kv1.6, and KCa), DTX-I (to block Kv1.1 and Kv1.6), DTX-K (to block Kv1.1 alone) and/or MgTX (to block Kv1.1, Kv1.3, and Kv1.6 but not Ca²⁺-activated K channels). Secreted cytokine was measured in culture supernatants 16 h after initial activation. In the absence of Kv channel blockers, stimulation led to the elaboration of a significant amount of IL-2 (208 pg/ml, n = 5), but production was decreased by CTX (127 pg/ml, n = 5) and DTX-I (179 pg/ml, n = 5) in CD3/CD28 primed naive CD4^{+} cells (39 and 14% inhibition, respectively; Fig. 8 A). The effect of MgTX was similar to that of CTX, and the Kv1.1-selective blocker DTX-K inhibited IL-2 production to a similar extent as did DTX-I (unpublished data). However, the combination of CTX and DTX-I inhibited IL-2 production (104 pg, n = 5) to a greater extent than did either blocker alone. Predictably, costimulatory blockade greatly decreased basal TCR-induced IL-2 levels (>50%; Fig. 8 B) and Kv channel inhibitors, except for the combination of CTX and DTX-I, induced little additional effect on IL-2 production on restimulation in the presence of CTLA-4 Ig.

Distinct Coupling of Kv Channels to Cytokine Production in Effector versus Anergic CD4^{+} T Cells. We also examined whether Kv channels regulate cytokine production during secondary responses of previously primed cells. CD4^{+} cells were first activated for 3 d in the presence of APCs with either CD3 and CD28, or CD3 and CTLA-4 Ig, and then rested for 24 h in fresh culture medium. IL-2, IFN-γ, and IL-4 levels were each measured after restimulation with plate-immobilized anti-CD3. None of the blockers exerted a significant effect on IL-2, IFN-γ, or IL-4 production by CD3/CD28 primed cells (Fig. 9 A), nor IL-2 or IFN-γ production during restimulation of CTLA-4 Ig-treated T cells (Fig. 9 B). Unexpectedly, pro-
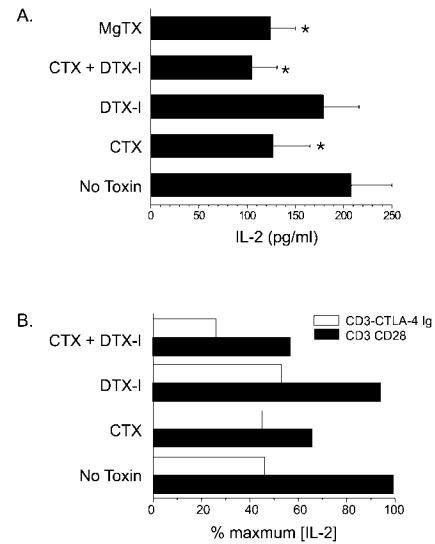
gressive inhibition of Kv channels in CTLA-4–treated lymphocytes induced a significant and graded augmentation of IL-4 production that suggests Kv channels normally act to suppress IL-4 production by anergic T cells. Thus, in addition to the well established requirement for Kv channel activity during primary responses of T cells, the repertoire of functions for Kv channels may also include a role in suppressing the transcription or elaboration of cytokines.

Distinct Regulation of Membrane Potential by Kv Channels in Naive, Effector, and Anergic CD4^{+} Lymphocytes. Previously, we demonstrated that IL-2 production by naive human T cells is modulated by changes in membrane voltage (9). Given the differences in Kv channel activity and the differential effects of Kv channel inhibitors on cytokine production by naive, effector, and anergic murine T cells, we directly measured Vm, and the contribution of each defined Kv current to the steady-state Vm in each of these T cell populations. The resting Vm was determined and then K⁺ channel inhibitors were added to selectively and sequentially inhibit different channel populations. DTX-I was applied first to block Kv1.1, Kv1.2, and Kv1.6, and then MgTX was added to block Kv1.3 channels. MgTX was used because, unlike CTX, it does not block calcium-activated potassium channels, which may contribute to the membrane potential. After MgTX addition, any effect of CTX would indicate that KCa channels have an active role in setting Vm. Representa-
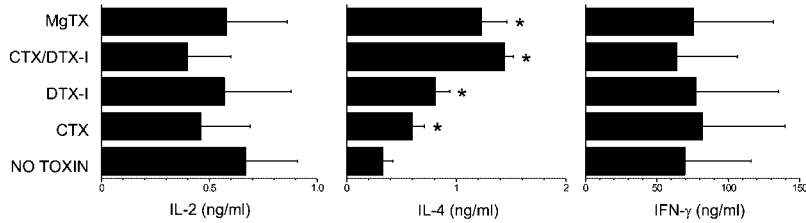
A. CD3/CD28 primed

B. CD3/CTLA-4 Ig primed

IL-2 (ng/ml)   IL-4 (ng/ml)   IFN-γ (ng/ml)
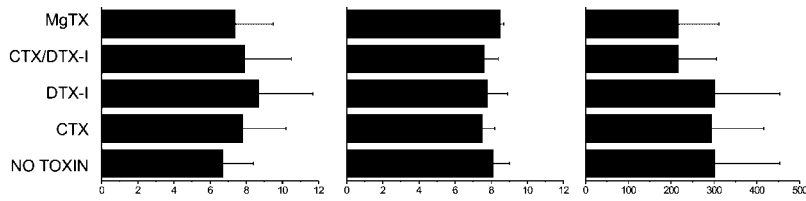
Figure 9. Effect of Kv channel blockade on IL-2, IL-4, and IFN-γ production by effector and anergic lymphocytes. Naive CD4$^+$ lymphocytes from C57Bl/6 mice were stimulated for 3 d in complete RPMI medium with (A) soluble 1 μg/ml αCD3 and 1 μg/ml αCD28 or (B) 1 μg/ml αCD3 and 10 μg/ml CTLA-4 Ig in the presence of APCs. Cells were collected, washed, and recultured in complete medium in the absence of any stimuli for 24 h and restimulated with plate-bound 1 μg/ml αCD3. Culture supernatants were collected between 16 and 18 h after restimulation and assayed for IL-2, IL-4, and IFN-γ as described. Toxins were added to cells at least 30 min before stimulation. All data represent the mean of (±SD) of at least three separate experiments, each performed in duplicate. When indicated the results are significantly different: *, P < 0.05.

tive examples of recordings obtained from naive, effector, and anergic CD4$^+$ lymphocytes, generated in vitro as described in Materials and Methods, are shown (Fig. 10). The results obtained from indicated numbers of individual cells and summarized in Table I demonstrate that the Vm of naive cells is regulated by each pharmacologically defined Kv current we identified in voltage-clamp experiments. DTX-I induces a small but consistent depolarization and MgTX an additional decrease in Vm to about −38 mV. The combination of DTX and MgTX blocks all Kv channels expressed in murine CD4+ T cells (demonstrated herein). Importantly, DTX-I and MgTX had virtually no effect (ΔVm < 5 mV) on the Vm of effector cells generated in vivo or in vitro (Fig. 10 and Table I). However, anergic cells, generated in vivo or in vitro, were sensitive to DTX-I. Anergic T cells produced in vitro by blocking costimulation were, however, somewhat different than cells anergized in vivo, in that they exhibited sensitivity to both DTX-I and MgTX. This difference may reflect the fact that in vivo anergized cells also exhibit less prominent time-dependent inactivation due to a more prominent effect of DTX-I (nonactivating) Kv channels on their phenotype.

Differential Regulation of Calcium Signaling by Kv Channels in Naive, Effector, and Anergic T Cells. The different role of Kv channels in regulating Vm of naive, effector, and anergic lymphocytes would be expected to directly impact TCR-mediated calcium influx because permeation of CRAC channels is highly membrane potential dependent. We used DTX-I and MgTX to determine whether membrane potential and calcium signaling are coordinately regulated by Kv channels in each distinct T cell population. Calcium was mobilized by cross-linking CD3 and CD4 with biotinylated mAb and streptavidin in the absence of blockers (Materials and Methods) or in the presence of DTX-I and MgTX. Stimulation of untreated cells induced an increase in [Ca^{2+}]$_i$ in naive cells that quickly reached a peak concentration (500–600 nM) and then decayed to an elevated steady-state level (∼350 nM) over several minutes. DTX-I treatment decreased the peak and plateau levels by ∼200 nM and MgTX exerted an even greater inhibitory effect (∼100 nM). Anergic cells exhibited a similar blocker profile as naive cells that is consistent with their effect on Vm. Significantly, calcium signals in effector cells, like Vm (Fig. 10), were not diminished by channel blockers, indicating that neither the membrane potential nor calcium is regulated by Kv channels in productively primed T lymphocytes.
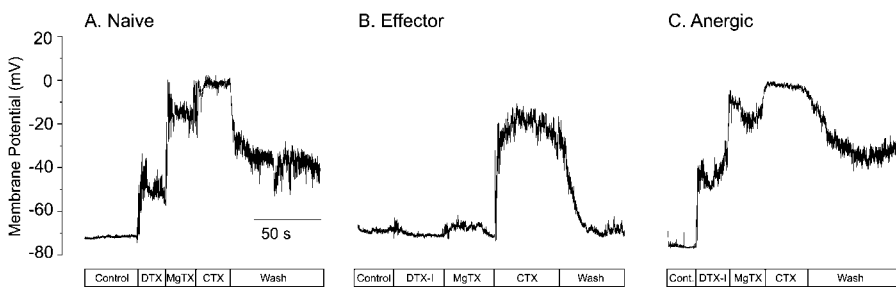

A. Naive   B. Effector   C. Anergic

50 s

Control DTX MgTX CTX Wash   Control DTX-I MgTX CTX Wash   Cont. DTX-I MgTX CTX Wash

Figure 10. Regulation of membrane potential by K$^+$ channels in naive, effector, and anergic CD4$^+$ lymphocytes. The membrane potential of naive, effector, and anergic CD4$^+$ lymphocytes was recorded using the current clamp mode of the patch-clamp recording technique. Representative traces are shown from naive CD4$^+$ lymphocytes, and effector and anergic cells produced in vitro from naive CD4$^+$ lymphocytes (C57Bl/6) stimulated with αCD3 plus αCD28 (B) or αCD3 and CTLA-4 Ig (C) and APCs. The resting steady-state Vm was recorded in each cell type and toxins (100 nm) were sequentially added (as indicated) to the recording chamber to determine the contribution of DTX-I–, MgTX-, and CTX-sensitive K$^+$ currents.

Table I. *Effect of K$^+$ Blockers on the Membrane Potential of CD4$^+$ T Cells*

	Naive	Effector	Anergic
Nontransgenic CD4$^+$ cells generated in vitro			
	−66 ± 8 mV	−54 ± 8 mV	−72 ± 1 mV
DTX-I	Δ13 ± 3 mV[a]	Δ0.4 ± 3 mV	Δ16 ± 5 mV
MgTX	Δ28 ± 5 mV	Δ4 ± 2 mV	Δ16 ± 4 mV
Vm[b]	−26 mV	−50 mV	−40 mV
CTX	Δ15 ± 2 mV	Δ29 ± 6 mV	Δ32 ± 4 mV
Vm[c]	−11 mV	−21 mV	−8 mV
n	5	5	7
Vβ8.1 TCR$^+$ CD4$^+$ cells generated in vivo			
	−65 ± 3 mV	−64 ± 2 mV	−66 ± 3 mV
DTX-I	Δ14 ± 3 mV	Δ0.8 ± 0.5 mV	Δ48 ± 5 mV
MgTX	Δ13 ± 3 mV	Δ4 ± 2 mV	Δ0 ± 0 mV
Vm[b]	−38 mV	−59 mV	−18 mV
CTX	Δ21 ± 3 mV	Δ33 ± 3 mV	Δ3.5 ± 4 mV
Vm[c]	−17 mV	−26 mV	−14 mV
n	20	20	4

[a]Mean change in membrane potential induced by each blocker is indicated (Δ).
[b]Calculated membrane potential in the presence of DTX-1 and MgTX.
[c]Calculated membrane potential in the presence of DTX-1, MgTX, and CTX.

Discussion

Voltage-gated potassium channels regulate physiological and immunological functions of T lymphocytes including adhesion molecule activation, the membrane potential, calcium influx, effector cytokine production, clonal expansion, and cell death. Because naive lymphocytes are multipotent, and their differentiation is modulated by dynamic interactions with antigen, costimulatory influences, and microenvironmental factors, we asked whether functional Kv channels (Kv currents), which are implicated in these many T cell functions and fates, are coordinately or dynamically regulated by the quality and quantity of priming in vitro and in vivo. In this paper, we have focused on the modulation of functional Kv channels (currents) by TCR and costimulatory signals, and the immunological roles of these channels. We have identified qualitative and quantitative changes in Kv currents that are linked to the differentiation state of peripheral murine CD4$^+$ lymphocytes. Naive CD4$^+$ lymphocytes express a CTX-sensitive current (Kv1.3) and a CTX-resistant DTX-I–sensitive current. Part of this DTX-I–sensitive current of naive and anergized T cells is also blocked by the Kv1.1 specific blocker DTX-K. The remaining DTX-K–resistant DTX-I–sensitive current is consistent with Kv1.2 and/or Kv1.6, both of which are expressed at the mRNA level. Impor-

tantly, we find that the amplitude and composition of Kv currents is regulated by the strength of TCR priming and the presence or absence of costimulation. Strong/productive priming (in vitro or in vivo) suppresses all DTX-sensitive Kv current and increases the amplitude of DTX-resistant, CTX-sensitive (Kv1.3) current as previously observed in mitogen-stimulated human and murine lymphocytes (18, 20). Incompletely primed/anergized CD4$^+$ cells, like productively primed cells, express increased levels of Kv1.3 current, but maintain relatively constant levels of DTX-K–(Kv1.1) and DTX-I–sensitive current (Kv1.2/Kv1.6).

Our in vivo and in vitro findings suggest that the quality of TCR and costimulatory signals coordinately regulates Kv channel expression/activity and CD4$^+$ lymphocyte differentiation. Productive TCR/CD3-mediated signals seem to be sufficient to induce an increase in Kv1.3 expression because both effector and anergic cells express more Kv1.3 current than naive cells. However, costimulatory signals, which appear to be mediated by CD28 stimulation, are required to initiate a decrease in DTX-sensitive Kv current, and to prevent the induction of anergy. This tight correspondence between Kv channel expression and CD4$^+$ lymphocyte differentiation suggests that distinct Kv current activities may support unique functions associated with each immunological state. In fact, our data indicate that Kv channels expressed by productively primed and anergized lymphocytes differentially regulate secondary (TCR–dependent) effector responses (cytokine production) of primed lymphocytes (Fig. 9).

One important function of regulated K$^+$ efflux is the production of an electronegative cell interior and a transmembrane electrical potential, which had been estimated to be about −60 to −70 mV using indirect methods (6, 39, 40). This electrical gradient is necessary for stimulated calcium influx, as the substantial inward concentration gradient is, remarkably, insufficient to drive Ca$_e^{2+}$ permeation of activated CRAC channels in the absence of the K$^+$ (channel) efflux-dependent membrane potential (8). Consequently, the degree of membrane hyperpolarization (intracellular negative charge) determines the magnitude of the Ca$_e^{2+}$ influx via CRAC channels (8). Because Kv channel inhibitors (DTX-I and/or MgTX) depolarize naive and anergic T cells, it is not surprising that they also attenuate TCR-mediated calcium signaling (Fig. 11). The effect on Vm and calcium signaling, although incomplete, is sufficient to affect cytokine production. In fact, we previously found significant inhibition of IL-2 production by human T cells occurred in response to relatively small depolarizations ($\sim$Δ25 mV; reference 9). Thus, the extent of Kv blocker–mediated depolarization (Δ30–50 mV) observed in naive and anergic T cells also appears to be sufficient to alter cytokine production by these populations. Nonetheless, a significant proportion of the membrane potential is not regulated by Kv channels, and calcium-activated K channels (41, 42) and electrogenic pathways such as the Na$^+$/K$^+$ ATPase (sodium pump; reference 43) expressed in T cells are likely responsible for this residual Vm.
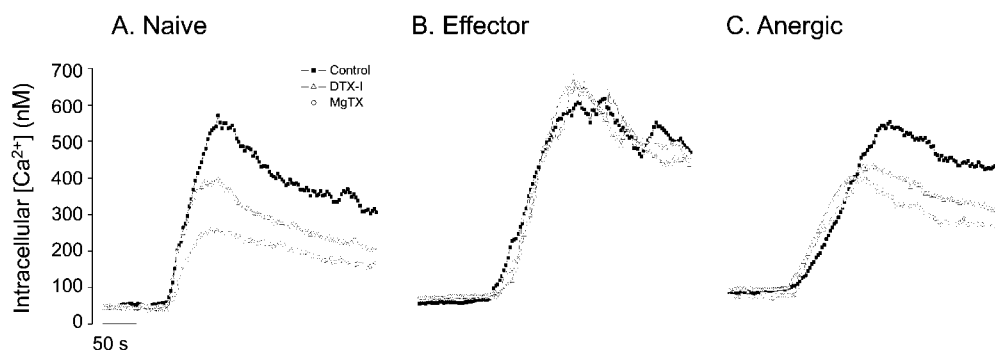
Figure 11. Regulation of calcium signaling by Kv channels in naive, effector and anergic CD4$^+$ lymphocytes. The intracellular calcium concentration was measured in naive (A), effector (B), and anergic (C) CD4$^+$ lymphocytes, which were generated in vitro as described in Materials and Methods. Each trace represents the average calcium concentration in at least 50 CD4$^+$ cells and calcium signals were initiated by cross-linking receptor bound biotin-conjugated αCD3 and αCD4 mAb with 1 μg/ml streptavidin. The effect of 100 nM DTX-I and 100 nM MgTX were determined in consecutive experiments on the same cell preparations and results shown are typical of three separate cell preparations for each population.

A surprising result of these studies is the augmentation of IL-4 production by Kv channel blockers in anergized CD4$^+$ lymphocytes. This finding suggests that a more complex repertoire of functions may exist for Kv channels during other immunological responses of T cells. In anergized cells, IL-4 augmentation by Kv channel inhibitors may reflect the fact that low amplitude calcium signals bias the cytokine profile toward the transcription/production of IL-4 (and not IL-2) via the differential activation of NFATc and NFATp (44). Thus, diminished calcium signaling in partially primed (anergic) T cells may be analogous to diminished (APL-like) calcium signaling, which has been shown to induce IL-4 production upon restimulation of incompletely primed cells.

Another unexpected finding was that Kv channels do not regulate secondary physiological and immunological responses of effector cells. Thus, although Kv1.3 expression is increased, Kv channels neither contribute significantly to the membrane potential, nor to calcium signaling and cytokine production. This consistent pattern of insensitivity to Kv blockers in effector cells provides an explanation for our perplexing results, but also those of in vivo studies which demonstrated that blockers suppressed primary responses to antigen (Ab production and DTH responses) in miniswine, and immune-mediated neurodegeneration during experimentally-induced allergic encephalitis in the rat during primary antigen exposure, but not secondary responses to a subsequent antigen challenge (21, 22).

The mere fact that Kv channels can uncouple from membrane potential in effector cells is an interesting paradox because it has been shown that overexpression of Kv1.3 channels (like that observed in effector cells) shifts (hyperpolarizes) the membrane potential of a nonlymphoid cell to that of naive T cells (45). In the context of our findings with effector cells, this result demonstrates that increased Kv1.3 expression alone is insufficient to establish coupling to Vm, and that posttranslational mechanisms may be involved or required. It is also possible that inherent differences in the biophysical properties of individual channel isoforms including the dominant effects of distinct subunits in heterotetramers play a role in this regulation. In fact, the Kv channel isoforms we have identified in T cells could produce an array of oligomeric channel structures that define a wide flexibility or diversity of physiological activities and immunological functions.

Although the oligomeric structure (subunit composition) of Kv channels cannot be determined with the patch clamp, the changes in Kv channel expression level and current kinetics we have observed in lymphocytes certainly reflect the aggregate phenotype of distinct populations of homooligomeric channels and/or the dominant phenotype of heterooligomeric structures. In addition to establishing a level of tonic activity, the oligomeric composition of lymphocyte Kv channels may also determine their sensitivity to dynamic (posttranslational) modifications, such as phosphorylation, which regulate Kv channel biophysical properties (46, 47). Thus, for example, IL-4 production and TH2 cell differentiation in vivo may be specifically enhanced if Kv channel activity is suppressed by intracellular signaling responses to external stimuli, by physiological variations in the ionic composition or tonicity of the external milieu at sites of activation or inflammation, or by TCR and CD28-regulated Kv channel expression and/or oligomerization. These signaling pathways that dynamically regulate Kv channel activity or affect their coupling to membrane potential and calcium signaling in naive, effector, and anergic T cells represent additional targets for Kv channel-mediated immune regulation. Therefore, future studies will address the mechanisms by which Kv currents are dynamically regulated in naive and primed cells and the consequences for immune function.

References

1. Freedman, B.D., B.K. Fleischmann, J.A. Punt, G. Gaulton, Y. Hashimoto, and M.I. Kotlikoff. 1995. Identification of Kv1.1 expression by murine CD4$^-$CD8$^-$ thymocytes. A role for voltage-dependent K$^+$ channels in murine thymocyte development. *J. Biol. Chem.* 270:22406–22411.

2. Lewis, R.S., and M.D. Cahalan. 1995. Potassium and calcium channels in lymphocytes. *Annu. Rev. Immunol.* 13:623–653.

3. Lewis, R.S., and M.D. Cahalan. 1989. Mitogen-induced oscillations of cytosolic Ca^{2+} and transmembrane Ca^{2+} current in human leukemic T cells. *Cell Regul.* 1:99–112.

4. Gelfand, E.W., R.K. Cheung, and S. Grinstein. 1984. Role of membrane potential in the regulation of lectin-induced calcium uptake. *J. Cell. Physiol.* 121:533–539.

5. Hess, S.D., M. Oortgiesen, and M.D. Cahalan. 1993. Calcium oscillations in human T and natural killer cells depend upon membrane potential and calcium influx. *J. Immunol.* 150:2620–2633.

6. Grinstein, S., and J.D. Smith. 1990. Calcium-independent cell volume regulation in human lymphocytes. Inhibition by charybdotoxin. *J. Gen. Physiol.* 95:97–120.

7. Lin, S.C., R.C. Boltz, J.T. Blake, M. Nguyen, A. Talento, P.A. Fischer, M.S. Springer, N.H. Sigal, R.S. Slaughter, M.L. Garcia, et al. 1993. Voltage-gated potassium channels regulate calcium-dependent pathways involved in human T lymphocyte activation. *J. Exp. Med.* 177:637–645.

8. Verheugen, J.A., and H. Korn. 1997. A charybdotoxin-insensitive conductance in human T lymphocytes: T cell membrane potential is set by distinct K$^+$ channels. *J. Physiol.* 503:317–331.

9. Freedman, B.D., M.A. Price, and C.J. Deutsch. 1992. Evidence for voltage modulation of IL-2 production in mitogen-stimulated human peripheral blood lymphocytes. *J. Immunol.* 149:3784–3794.

10. Leonard, R.J., M.L. Garcia, R.S. Slaughter, and J.P. Reuben. 1992. Selective blockers of voltage-gated K$^+$ channels depolarize human T lymphocytes: mechanism of the antiproliferative effect of charybdotoxin. *Proc. Natl. Acad. Sci. USA.* 89:10094–10098.

11. Vu, C.C., C.D. Bortner, and J.A. Cidlowski. 2001. Differential involvement of initiator caspases in apoptotic volume decrease and potassium efflux during fas- and UV-induced cell death. *J. Biol. Chem.* 276:37602–37611.

12. Bortner, C.D., and J.A. Cidlowski. 1999. Caspase independent/dependent regulation of K$^+$, cell shrinkage, and mitochondrial membrane potential during lymphocyte apoptosis. *J. Biol. Chem.* 274:21953–21962.

13. Maeno, E., Y. Ishizaki, T. Kanaseki, A. Hazama, and Y. Okada. 2000. Normotonic cell shrinkage because of disordered volume regulation is an early prerequisite to apoptosis. *Proc. Natl. Acad. Sci. USA.* 97:9487–9492.

14. Levite, M., L. Cahalon, A. Peretz, R. Hershkoviz, A. Sobko, A. Ariel, R. Desai, B. Attali, and O. Lider. 2000. Extracellular K$^+$ and opening of voltage-gated potassium channels activate T cell integrin function: physical and functional association between Kv1.3 channels and β1 integrins. *J. Exp. Med.* 191:1167–1176.

15. Lewis, R.S., and M.D. Cahalan. 1988. Subset-specific expression of potassium channels in developing murine T lymphocytes. *Science.* 239:771–775.

16. McKinnon, D., and R. Ceredig. 1986. Changes in the expression of potassium channels during mouse T cell development. *J. Exp. Med.* 164:1846–1861.

17. DeCoursey, T.E., K.G. Chandy, S. Gupta, and M.D. Cahalan. 1987. Two types of potassium channels in murine T lymphocytes. *J. Gen. Physiol.* 89:379–404.

18. Deutsch, C., D. Krause, and S.C. Lee. 1986. Voltage-gated potassium conductance in human T lymphocytes stimulated with phorbol ester. *J. Physiol.* 372:405–423.

19. DeCoursey, T.E., K.G. Chandy, S. Gupta, and M.D. Cahalan. 1987. Mitogen induction of ion channels in murine T lymphocytes. *J. Gen. Physiol.* 89:405–420.

20. Lee, S.C., D.E. Sabath, C. Deutsch, and M.B. Prystowsky. 1986. Increased voltage-gated potassium conductance during interleukin 2-stimulated proliferation of a mouse helper T lymphocyte clone. *J. Cell Biol.* 102:1200–1208.

21. Koo, G.C., J.T. Blake, A. Talento, M. Nguyen, S. Lin, A. Sirotina, K. Shah, K. Mulvany, D. Hora, Jr., P. Cunningham, et al. 1997. Blockade of the voltage-gated potassium channel Kv1.3 inhibits immune responses in vivo. *J. Immunol.* 158:5120–5128.

22. Beeton, C., J. Barbaria, P. Giraud, J. Devaux, A.M. Benoliel, M. Gola, J.M. Sabatier, D. Bernard, M. Crest, and E. Beraud. 2001. Selective blocking of voltage-gated K$^+$ channels improves experimental autoimmune encephalomyelitis and inhibits T cell activation. *J. Immunol.* 166:936–944.

23. Beeton, C., H. Wulff, J. Barbaria, O. Clot-Faybesse, M. Pennington, D. Bernard, M.D. Cahalan, K.G. Chandy, and E. Beraud. 2001. Selective blockade of T lymphocyte K$^+$ channels ameliorates experimental autoimmune encephalomyelitis, a model for multiple sclerosis. *Proc. Natl. Acad. Sci. USA.* 98:13942–13947.

24. Yui, K., S. Komori, M. Katsumata, R. Siegel, and M.I. Greene. 1990. Self-reactive T cells escape clonal deletion in T-cell receptor Vβ8.1 transgenic mice. *Proc. Natl. Acad. Sci. USA.* 87:7135–7139.

25. Bhandoola, A., E.A. Cho, K. Yui, H.U. Saragovi, M.I. Greene, and H. Quill. 1993. Reduced CD3-mediated protein tyrosine phosphorylation in anergic CD4$^+$ and CD8$^+$ T cells. *J. Immunol.* 151:2355–2367.

26. Wells, A.D., H. Gudmundsdottir, and L.A. Turka. 1997. Following the fate of individual T cells throughout activation and clonal expansion. Signals from T cell receptor and CD28 differentially regulate the induction and duration of a proliferative response. *J. Clin. Invest.* 100:3173–3183.

27. Hayakawa, K., and R.R. Hardy. 1988. Murine CD4$^+$ T cell subsets defined. *J. Exp. Med.* 168:1825–1838.

28. Hayakawa, K., and R.R. Hardy. 1989. Phenotypic and functional alteration of CD4$^+$ T cells after antigen stimulation. Resolution of two populations of memory T cells that both secrete interleukin 4. *J. Exp. Med.* 169:2245–2250.

29. Garcia, M.L., M. Garcia-Calvo, P. Hidalgo, A. Lee, and R. MacKinnon. 1994. Purification and characterization of three inhibitors of voltage-dependent K$+$ channels from *Leirus quinquestriatus* var. hebraeus venom. *Biochemistry.* 33:6834–6839.

30. Grissmer, S., A.N. Nguyen, J. Aiyar, D.C. Hanson, R.J. Mather, G.A. Gutman, M.J. Karmilowicz, D.D. Auperin, and K.G. Chandy. 1994. Pharmacological characterization of five cloned voltage-gated K$+$ channels, types Kv1.1, 1.2, 1.3, 1.5, and 3.1, stably expressed in mammalian cell lines. *Mol. Pharmacol.* 45:1227–1234.

31. Hopkins, W.F., V. Demas, and B.L. Tempel. 1994. Both N- and C-terminal regions contribute to the assembly and func-

tional expression of homo- and heteromultimeric voltage-gated K+ channels. *J. Neurosci.* 14:1385–1393.

32. Robertson, B., D. Owen, J. Stow, C. Butler, and C. Newland. 1996. Novel effects of dendrotoxin homologues on subtypes of mammalian Kv1 potassium channels expressed in *Xenopus* oocytes. *FEBS Lett.* 383:26–30.

33. Grynkiewicz, G., M. Poenie, and R.Y. Tsien. 1985. A new generation of Ca²⁺ indicators with greatly improved fluorescence properties. *J. Biol. Chem.* 260:3440–3450.

34. Chomczynski, P., and N. Sacchi. 1987. Single-step method of RNA isolation by acid guanidinium thiocyanate-phenol-chloroform extraction. *Anal. Biochem.* 162:156–159.

35. Tempel, B.L., D.M. Papazian, T.L. Schwarz, Y.N. Jan, and L.Y. Jan. 1987. Sequence of a probable potassium channel component encoded at the Shaker locus of *Drosophila*. *Science.* 237:770–775.

36. Roberds, S.L., and M.M. Tamkun. 1991. Cloning and tissue-specific expression of five voltage-gated potassium channel cDNAs expressed in rat heart. *Proc. Natl. Acad. Sci. USA.* 88:1798–1802.

37. Swanson, R., J. Marshall, J.S. Smith, J.B. Williams, M.B. Boyle, K. Folander, C.J. Luneau, J. Antanavage, C. Oliva, and S.A. Buhrow. 1990. Cloning and expression of cDNA and genomic clones encoding three delayed rectifier potassium channels in rat brain. *Neuron.* 4:929–939.

38. Maier, C.C., A. Bhandoola, W. Borden, K. Yui, K. Hayakawa, and M.I. Greene. 1998. Unique molecular surface features of in vivo tolerized T cells. *Proc. Natl. Acad. Sci. USA.* 95:4499–4503.

39. Grinstein, S., and J.D. Smith. 1989. Ca²⁺ induces charybdotoxin-sensitive membrane potential changes in rat lymphocytes. *Am. J. Physiol.* 257:C197–C206.

40. Rader, R.K., L.E. Kahn, G.D. Anderson, C.L. Martin, K.S. Chinn, and S.A. Gregory. 1996. T cell activation is regulated by voltage-dependent and calcium-activated potassium chan-

nels. *J. Immunol.* 156:1425–1430.

41. Khanna, R., M.C. Chang, W.J. Joiner, L.K. Kaczmarek, and L.C. Schlichter. 1999. hSK4/hIK1, a calmodulin-binding KCa channel in human T lymphocytes. Roles in proliferation and volume regulation. *J. Biol. Chem.* 274:14838–14849.

42. Logsdon, N.J., J. Kang, J.A. Togo, E.P. Christian, and J. Aiyar. 1997. A novel gene, hKCa4, encodes the calcium-activated potassium channel in human T lymphocytes. *J. Biol. Chem.* 272:32723–32726.

43. Ishida, Y., and T.M. Chused. 1993. Lack of voltage sensitive potassium channels and generation of membrane potential by sodium potassium ATPase in murine T lymphocytes. *J. Immunol.* 151:610–620.

44. Brogdon, J.L., D. Leitenberg, and K. Bottomly. 2002. The potency of TCR signaling differentially regulates NFATc/p activity and early IL-4 transcription in naive CD4(+) T cells. *J. Immunol.* 168:3825–3832.

45. Defarias, F.P., S.P. Stevens, and R.J. Leonard. 1995. Stable expression of human Kv1.3 potassium channels resets the resting membrane potential of cultured mammalian cells. *Receptors Channels.* 3:273–281.

46. Chang, M.C., R. Khanna, and L.C. Schlichter. 2001. Regulation of Kv1.3 channels in activated human T lymphocytes by Ca²⁺-dependent pathways. *Cell. Physiol. Biochem.* 11:123–134.

47. Szabo, I., E. Gulbins, H. Apfel, X. Zhang, P. Barth, A.E. Busch, K. Schlottmann, O. Pongs, and F. Lang. 1996. Tyrosine phosphorylation-dependent suppression of a voltage-gated K+ channel in T lymphocytes upon Fas stimulation. *J. Biol. Chem.* 271:20465–20469.

48. Chandy, K.G., C.B. Williams, R.H. Spencer, B.A. Aguilar, S. Ghanshani, B.L. Tempel, and G.A. Gutman. 1990. A family of three mouse potassium channel genes with intronless coding regions. *Science.* 247:973–975.